

Dinitrogen Labile Coordination versus Four-Electron Reduction, THF Cleavage, and Fragmentation Promoted by a (calix-tetrapyrrole)Sm(II) Complex

Jingwen Guan, Tiffany Dubé, Sandro Gambarotta,* and Glenn P. A. Yap

Department of Chemistry, University of Ottawa, Ottawa, Ontario, K1N 6N5, Canada

Received August 11, 2000

A divalent calix-tetrapyrrole Sm complex, $\{[(-CH_2-)_5]_4\text{-calix-tetrapyrrole}\}\text{Sm}(\text{THF})[\text{Li}(\text{THF})]_2[\text{Li}(\text{THF})_2](\mu^3\text{-Cl})$ (**1**), reacts with dinitrogen to reversibly form the labile dinuclear complex $\{[(-CH_2-)_5]_4\text{-calix-tetrapyrrole}\}\text{Sm}[\text{Li}(\text{THF})]_3(\mu^3\text{-Cl})_2(\mu^2\text{-N}_2)\cdot 2\text{THF}$ (**2**). Further attack on **2** by two additional molecules of **1** afforded four-electron reduction of the coordinated dinitrogen and formation of the novel trinuclear dinitrogen complex $\{[(-CH_2-)_5]_4\text{-calix-tetrapyrrole}\}_2\text{Sm}_3\text{Li}_2(\mu^3\text{-N}_2)[\text{Li}(\text{THF})_2]\cdot\text{THF}$ (**5**). The formation of this species, where one calix-tetrapyrrole ligand was abstracted from one of the three samarium centers, is accompanied by formation of $\{[(-CH_2-)_5]_4\text{-calix-tetrapyrrole}\}[\text{Li}(\text{THF})]_4$ (**6**) and of the trivalent $\{[(-CH_2-)_5]_4\text{-calix-tetrapyrrole}\}\text{Sm}(\text{Cl})\{[\text{Li}(\text{THF})]_3(\mu^3\text{-Cl})\}$ (**7**). A THF degradation reaction occurs in parallel to the dinitrogen fixation process. During the formation of **2**, complex **1** also reacts with THF to afford another mononuclear divalent Sm complex, $\{[(-CH_2-)_5]_4\text{-calix-tetrapyrrole}\}\text{Sm}(\text{THF})\text{Li}_2[\text{Li}(\text{THF})](\mu^3\text{-OCH=CH}_2)$ (**3**). This species contains an enolate fragment in the molecular backbone and shows no reactivity with N_2 . Recrystallization of **3** from THF did not eliminate the enolate fragment but afforded instead another divalent complex, $\{[(-CH_2-)_5]_4\text{-calix-tetrapyrrole}\}\text{Sm}(\text{THF})_2\{\text{Li}[\text{Li}(\text{THF})]_2\}(\mu^3\text{-OCH=CH}_2)\cdot\text{THF}$ (**4**), also unreactive toward N_2 . Finally a slow THF deoxygenation process occurs during the formation of **2** and **5**, affording a dinuclear trivalent oxo derivative $\{[(-CH_2-)_5]_4\text{-calix-tetrapyrrole}\}\text{Sm}[\text{Li}(\text{THF})]_3(\mu^3\text{-Cl})_2(\mu\text{-O})$ (**8**).

Introduction

The ability of divalent samarium to systematically perform multielectron reductions via cooperative attack of two or more metal centers on the same substrate is one of the distinctive characteristics of its reactivity. The complexity and variety of the transformations discovered for the samarocene derivatives (e.g., CO oligomerization,¹ the complex pattern of reactivity with alkynes,² insertion reactions³) are indeed a direct consequence of this unique behavior.

The reactivity of divalent samarium with dinitrogen seems to follow the same trend. The first example of a lanthanide dinitrogen complex was reported by Evans with the isolation of a dinuclear decamethylsamarocene side-on dinitrogen complex.⁴ The labile coordination corresponded in this case to an unusually short N–N distance indicative of minimal perturbation of the N–N triple bond. On the opposite extreme, an in situ generated Sm(II) calix-tetrapyrrole derivative has afforded a four-electron reduction and formation of the dinuclear

$\{(\text{Et}_8\text{-calix-tetrapyrrole})\text{SmLi}\}_2\text{Li}_4\text{N}_2$ complex.⁵ Given that a divalent samarium center may act only as a one-electron reductant, the formation of this species necessarily implies that a cooperative action of four metal centers occurred at some stage. Gathering four bulky complexes around the same small N_2 molecule certainly is an entropically disfavored event. Nevertheless, evidence for this possibility was recently obtained with the isolation of a tetranuclear samarium dinitrogen complex of a related ligand system where the coordinated dinitrogen has also undergone a four-electron reduction.⁶

One of the goals of this study was to attempt to understand the four-electron reduction of dinitrogen that occurred during the formation of the dinuclear $\{(\text{Et}_8\text{-calix-tetrapyrrole})\text{SmLi}\}_2\text{Li}_4\text{N}_2$ complex containing a $[\text{N}_2]^{4-}$ unit in a Sm_2Li_4 cage.⁵ We were also interested in elucidating the ligand features that triggered the reactivity with dinitrogen. It should be reiterated that a common feature among the three existing dinitrogen samarium complexes is the presence of a bent-metallocene type of geometry provided to the metal by the well-diversified ligand systems. Conversely, all the other existing divalent samarium complexes reported to date (alkoxides, amide, phosphide, etc.)⁷ do not display reactivity with N_2 . Furthermore, we have recently observed that the same $(\text{Et}_8\text{-calix-tetrapyrrole})\text{Sm}(\text{II})$

(1) Evans, W. J.; Grate, J. W.; Hughes, L. A.; Zhang, H.; Atwood, J. L. *J. Am. Chem. Soc.* **1985**, *107*, 3728.

(2) Evans, W. J.; Rabe, G. W.; Ziller, J. W. *J. Organomet. Chem.* **1994**, *483*, 21. (b) Evans, W. J.; Keyer, R.; Ziller, J. W. *Organometallics* **1993**, *12*, 2618. (c) Evans, W. J.; Keyer, R.; Ziller, J. W. *Organometallics* **1990**, *9*, 2628.

(3) (a) Evans, W. J.; Hughes, L. A.; Drummond, D. K.; Zhang, H.; Atwood, J. L. *J. Am. Chem. Soc.* **1986**, *108*, 1722. (b) Evans, W. J.; Drummond, D. K.; *J. Am. Chem. Soc.* **1988**, *110*, 2772.

(4) Evans, W. J.; Ulibarri, T. A.; Ziller, J. W. *J. Am. Chem. Soc.* **1988**, *110*, 6877.

(5) Jubb, J.; Gambarotta, S. *J. Am. Chem. Soc.* **1994**, *116*, 4477.

(6) Dubé, T.; Conoci, S.; Gambarotta, S.; Yap, G. P. A.; Vasapollo, G. *Angew. Chem., Int. Ed.* **1999**, *38*, 3657.

(7) Edelmann, F. In *Comprehensive Organometallic Chemistry*, 2nd ed.; Wilkinson, G., Ed.; Pergamon Press: Oxford, 1995.

complex that gave *irreversible* dinitrogen encapsulation is also capable of *reversibly* coordinating a molecule of ethylene in a side-on fashion.⁸ The reversibility of the ethylene fixation was rather surprising considering that dinitrogen is a substrate notoriously more difficult than ethylene to be reduced. In addition, the ability of the calix-tetrapyrrole samarium complexes to interact with ethylene was greatly sensitive to relatively minor variations in both the macrocycle substituents and the nature of additional groups (LiO-CH=CH₂ versus LiCl) coordinated to the ligand backbone. These observations prompted us to revisit the dinitrogen activation process in divalent samarium calix-tetrapyrrole chemistry with the help of the {[(−CH₂−)₅]₄-calix-tetrapyrrole}^{4−} tetra-anion.⁹ Herein we describe our observations.

Experimental Section

All operations were performed under an inert atmosphere of a nitrogen-filled drybox or by using standard Schenk-type glassware in combination with a nitrogen vacuum line. SmCl₃·(THF)₃,¹⁰ SmI₂(THF)₂,¹¹ and the {[(−CH₂−)₅]₄-calix-tetrapyrrole}⁹ {[(−CH₂−)₅]₄-calix-tetrapyrrole}Sm(THF)[Li(THF)]₂·[Li(THF)]₂(μ³-Cl) (**1**)¹² were prepared according to literature procedures. C₆D₆ and THF-*d*₈ were dried over Na/K alloy, vacuum-transferred into ampules, and stored under nitrogen prior to use. Infrared spectra were recorded on a Mattson 3000 FTIR instrument from Nujol mulls or KBr pellets prepared inside the drybox. Samples for magnetic susceptibility measurements were carried out at room temperature using a Gouy balance (Johnson Matthey). Magnetic moments were calculated by following standard methods,¹³ and corrections for underlying diamagnetism were applied to the data.¹⁴ Elemental analyses were carried out using a Perkin-Elmer Series II CHN/O 2400-analyzer.

Preparation of {[(−CH₂−)₅]₄-calix-tetrapyrrole}Sm-[Li(THF)]₃(μ³-Cl)₂(μ-N₂)·2THF (2**).** A deep green solution of **1** (4.5 g, 3.9 mmol) in freshly distilled THF (50 mL), maintained under an atmosphere of Ar, was concentrated to small volume (5 mL). Hexane (200 mL) was added, and the resulting suspension was heated to 60 °C until most of the dark green solid was dissolved. The hot solution was filtered to remove a small amount of insoluble solid. After cooling to room temperature, the solution was exposed to N₂ and was allowed to stand at room temperature. After 2 days, a red crystalline mass containing a mixture of **2** and **3** separated (2.1 g). Analytically pure samples of **2** for combustion analysis and spectroscopic characterization were obtained by separating the crystals of different shape using a stereomicroscope. IR (Nujol mull, cm^{−1}): ν: 3095(w), 3076(w), 2729(w), 2684(w), 1645(w), 1458(s), 1377(s), 1342(m), 1273(m), 1261(s), 1232(w), 1151(w), 1105(m,br), 1047(s), 980(m), 897(m), 876(m), 804(s), 771(w), 733(m), 704(w). El. Anal. Calcd (Found) for C₁₁₂H₁₆₀N₁₀O₈Sm₂Cl₂Li₆: C 61.48 (61.33), H 7.37 (7.28), N 6.40 (6.31). μ_{eff} = 2.82 μ_B (per formula unit).

Preparation of {[(−CH₂−)₅]₄-calix-tetrapyrrole}Sm-(THF)Li₂[Li(THF)](μ³-OCH=CH₂) (3**).** A solid sample of **1** (18.4 g, 16 mmol) was pumped in vacuo for 1 h. The dark residue was washed with two portions of ether and then redissolved in toluene (100 mL). The dark green solution was filtered to eliminate a small amount of insoluble, lightly colored residue, concentrated to small volume, and allowed to stand at room temperature for 2 days. Dark red crystals of **3** (7.1 g, 7.5 mmol, yield 47%) were obtained. Anal. Calcd (Found) for C₅₀H₆₇Li₃N₄O₃Sm: C 63.66 (63.22), H 7.16 (7.36), N 5.94 (5.92). IR (Nujol mull, cm^{−1}): ν: 1446(vs), 1365(vs), 1343(s), 1286(s), 1272(s), 1260(s), 1235(m,br), 1186(s), 1134(s), 1106(s,sh), 1042(vs, br), 990(m, br), 969(w), 931(w), 917(w), 902(vs, br), 877(vs, sh), 832(s, sh), 796(s, sh), 769(vs), 755(vs), 737(vs), 670(w), 584(w). μ_{eff} = 3.57 μ_B.

Preparation of {[(−CH₂−)₅]₄-calix-tetrapyrrole}Sm-(THF)₂[Li[Li(THF)]₂](μ³-OCH=CH₂)·THF (4**).** A sample of red crystalline **3** (5.0 g, 5.3 mmol) was dissolved in a mixture of THF (60 mL) and hexane (40 mL) at room temperature. Upon standing at room temperature for two weeks, pale yellow crystals of **4** separated (4.1 g, 3.5 mmol, 66%). Anal. Calcd (Found) for C₆₂H₉₁Li₃N₄O₆Sm: C 63.71 (64.25), H 7.83 (7.85), N 4.76 (4.83). IR (Nujol mull, cm^{−1}): ν: 1579(w), 1464(s), 1446(vs), 1377(vs), 1365(s), 1343(s), 1287(s), 1272(s), 1260(s), 1235(s), 1186(s), 1134(s), 1106(m), 1042(vs), 990(m), 969(m), 931(m), 902(vs), 877(vs), 832(s, sh), 796(s), 769(vs), 670(m), 584(m). μ_{eff} = 3.23 μ_B.

Preparation of {[(−CH₂−)₅]₄-calix-tetrapyrrole}₂Sm₃Li₂[(μ-N₂)[Li(THF)]₂]·THF (5**).** When a dark green solution of **1** (2.0 g, 1.7 mmol) in THF (50 mL) was concentrated to small volume and allowed to stand at room temperature under nitrogen for a few days, an orange-red crystalline mass was obtained. The solid was filtered and washed with warm toluene to eliminate a small amount of dark green crystalline **1** (identified by X-ray diffraction). Recrystallization from boiling THF/toluene mixture followed by addition of hexane yielded analytically pure orange-red crystals of **5** (0.6 g, 0.3 mmol, 53%). Anal. Calcd (Found) for C₉₂H₁₂₀Li₃N₁₀O₃Sm₃: C 58.59 (58.43), H 6.41 (6.36), N 7.43 (7.42). IR (Nujol mull, cm^{−1}): ν: 1366(m), 1345(m), 1260(s), 1245(m), 1175(w), 1145(w), 1100(w, br), 1039(vs, br), 979(m), 894(m), 876(s), 833(m), 809(s), 770(vs, sh), 741(s, sh), 723(s), 703(w), 664(w). μ_{eff} = 2.94 μ_B (per formula unit).

Isolation of {[(−CH₂−)₅]₄-calix-tetrapyrrole}[Li(THF)]₄ (6**).** The THF mother liquor from the above preparation was concentrated to very small volume (about 10 mL) and treated with hexane (70 mL). A colorless solid separated, which was recrystallized from THF, yielding colorless pyrophoric crystals of **6** (0.23 g, 0.25 mmol, 15%). The extreme sensitivity prevented analytical characterization.

Preparation of {[(−CH₂−)₅]₄-calix-tetrapyrrole}Sm-(Cl)[Li(THF)]₃(μ³-Cl) (7**).** A suspension of SmCl₃(THF)₃ (7.7 g, 16.2 mmol) in THF (150 mL) was reacted with **6** (14.6 g, 16.2 mmol) at room temperature. The color of the resulting clear solution was pale greenish-yellow. After standing a few hours at room temperature, the solution was concentrated to small volume and layered with hexane. Pale greenish-yellow crystals of **7** separated upon standing at room temperature for 3 days (14 g, 13.4 mmol, 83%). Anal. Calcd (Found) for C₅₂H₇₂Li₃N₄O₃SmCl₂: C 59.86 (59.17), H 6.96 (6.94), N 5.37 (5.02). IR (Nujol mull, cm^{−1}): ν: 1601(s), 1499(w), 1459(vs), 1376(s), 1365(s), 1343(m), 1310(m), 1297(m), 1270(m), 1260(m), 1217(s), 1182(w), 1141(m), 1128(m), 1050(vs), 991(s), 900(s), 875(s), 832(m), 778(s), 737(s), 698(w), 681(m), 665(m), 599(m), 576(m), 559(w). μ_{eff} = 1.54 μ_B.

Isolation of {[(−CH₂−)₅]₄-calix-tetrapyrrole}Sm[Li-(THF)]₃(μ³-Cl)₂(μ-O) (8**).** The mother liquor of a preparation of either **2** or **5** was evaporated to dryness. The solid residue (about 8.0 g) was transferred to a Soxhlet extractor and separately extracted with boiling hexane, toluene, and THF. The pale green color of the THF extracts slowly faded at room

(8) Dubé, T.; Gambarotta, S.; Yap, G. P. A. *Angew. Chem., Int. Ed.* **1999**, *38*, 1432.

(9) Brown, W. H.; Hutchinson, B. J.; McKinnon, M. H. *Can. J. Chem.* **1971**, *49*, 4017.

(10) Anhydrous SmCl₃ was prepared following a standard procedure: (a) Freeman, J. H.; Smith, M. L. *J. Inorg. Nucl. Chem.*, **1958**, *7*, 224, and was transformed into the corresponding tetrahydrofuranate. (b) Manzer, L. E. *Inorg. Synth.* **1982**, *21*, 135.

(11) Evans, W. J.; Grate, J. W.; Choi, H. W.; Bloom, I.; Hunter, W. E.; Atwood, J. L. *J. Am. Chem. Soc.*, **1985**, *107*, 941.

(12) Dubé, T.; Gambarotta, S.; Yap, G. P. A. *Organometallics* **2000**, *19*, 121.

(13) Mabbs, M. B.; Machin, D.; *Magnetism and Transition Metal Complexes*; Chapman and Hall: London, 1973.

(14) Foese, G.; Gorter, C. J.; Smits, L. J. *Constantes Selectionnes, Diamagnetisme, Paramagnetisme Relaxation Paramagnetique*; Masson: Paris, 1957.

temperature within 2 weeks and colorless crystals of **8** separated (3.0 g, 0.5 mmol). Anal. Calcd (Found) for $C_{104}H_{144}Li_6N_8O_7Sm_2Cl_2$: C 61.48 (61.06), H 7.14 (6.99), N 5.52 (5.50). IR (Nujol mull, cm^{-1}): ν : 0.1460(vs), 1377(vs), 1366(w), 1341(w), 1296(m), 1261(m), 1180(w), 1139(w), 1046(s), 988(w), 968(w), 895(m), 875(m), 831(m), 775(s), 762(s), 722(s), 697(w), 653(s). $\mu_{eff} = 2.28 \mu_B$ per formula unit.

X-ray Crystallography. Suitable crystals were selected, mounted on thin glass fibers using viscous oil, and cooled to the data collection temperature. Despite several attempts at recrystallization for **2**, only poor quality crystals can be obtained, and the results presented represent the best efforts. Data were collected on a Bruker AX SMART 1k CCD diffractometer using $0.3^\circ \omega$ -scans at 0° , 90° , and 180° in ϕ . Unit-cell parameters were determined from 60 data frames collected at different sections of the Ewald sphere. Semiempirical absorption corrections based on equivalent reflections were applied to the data. Systematic absences in the diffraction data and unit-cell parameters were uniquely consistent for the reported space groups for **2**, **3**, **4**, **5**, **6**, and **7** and consistent for space groups $C2/c$ and Cc for **8**. Solution in the centric space group for **8** yielded chemically reasonable and computationally stable results of refinement. The compound molecules of **2**, **6**, and **8** are located on a 2-fold axis, an inversion center, and a 4-fold rotoinversion axis, respectively. A molecule of THF solvent was found cocrystallized in the asymmetric units of **2** and **4**. Attempts to model several peaks in the penultimate, difference electron density map in **5**, located away from the compound molecule, as a reasonable solvent molecule failed, and these apparent solvent atoms were arbitrarily assigned carbon atom identities at full occupancies. Because of the poor quality of the data crystal in **2**, only the samarium, lithium, chloride, and oxygen atoms could be refined anisotropically. In the remaining structures, all non-hydrogen atoms were refined with anisotropic displacement parameters. All hydrogen atoms were treated as idealized contributions. All scattering factors and anomalous dispersion factors are contained in the SHEXTL 5.10 program library (Sheldrick, G. M., Bruker AXS, Madison, WI, 1997). Selected crystal data and bond distances and angles for all the structures are given in Tables 1 and 2, respectively.

Results and Discussion

Solutions of $\{[(-CH_2)_5]_4\text{-calix-tetrapyrrole}\}Sm(THF)\cdot[Li(THF)]_2[Li(THF)_2](\mu^3\text{-Cl})$ (**1**)¹² in THF are stable while stored under Ar. However, when a dark green solution of **1** in a hexane/THF mixture was boiled and allowed to stand at room temperature under nitrogen gas for 2 days, a dark red crystalline mass separated from the green mother liquor (Scheme 1). A visual inspection showed that the crystalline red mass was composed of two different compounds, one minor (**2**) and one major (**3**), of similar color but with distinctively different shapes (rectangular versus hexagonal prisms). The two components of the red crystalline mixture were physically separated according to their different crystal shape and characterized. Both types of crystals were extremely air-sensitive and independently generated *dark green* solutions upon dissolving in ether or THF. In the case of **2** however, the dissolution process was accompanied by N_2 evolution (85% recovered with a Toepler pump), thus indicating the presence of labile coordination of dinitrogen in this species. No spontaneous decomposition was observed in solid state.

The labile coordination of N_2 rendered particularly difficult the preparation of crystalline samples of **2** suitable for X-ray diffraction. Nevertheless, in one case

Table 1. Crystal Data and Structure Analysis Results

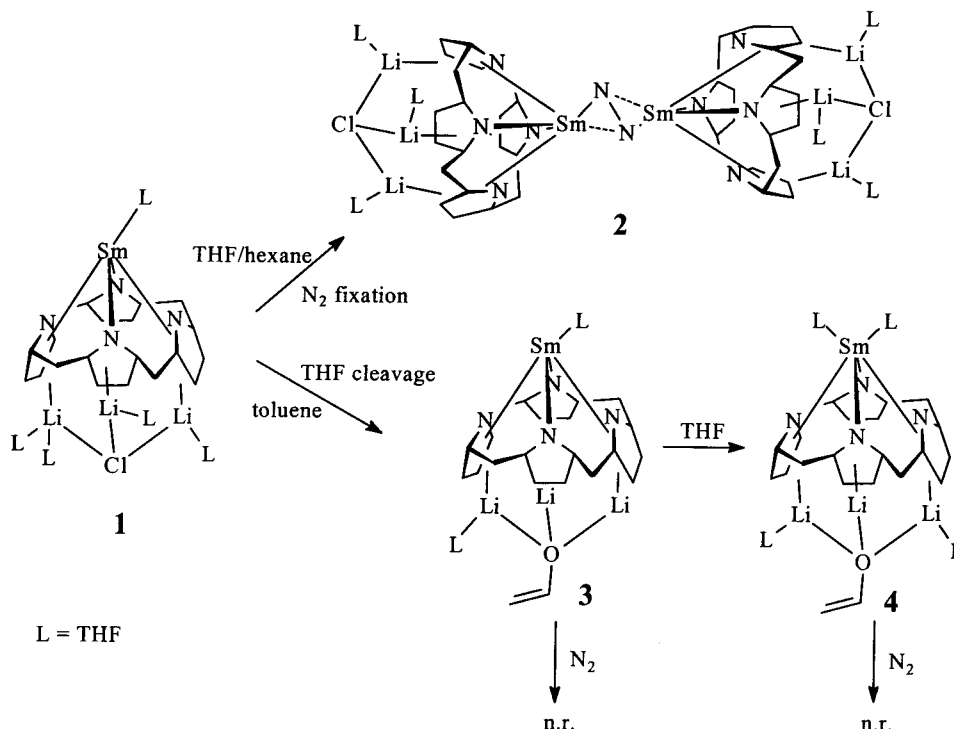
	2	3	4	5	6	7	8
formula	$C_{112}H_{160}Cl_2Li_6N_{10}O_8Sm_2$	$C_{50}H_{67}Li_3N_4O_3Sm$	$C_{62}H_{91}Li_3N_4O_6Sm$	$C_{88}H_{112}Li_3N_{10}O_2Sm_3\cdot THF$	$C_{58}H_{76}Li_4N_4O_4$	$C_{52}H_{72}Cl_2Li_3N_4O_3Sm$	$C_{104}H_{144}Cl_2Li_6N_8O_7Sm_2$
fw	2187.74	943.25	1159.56	1886.06	896.97	1043.21	2031.51
space group	monoclinic, $P2(1)/n$	monoclinic, $P2(1)/c$	monoclinic, $P2(1)/c$	monoclinic, $P2(1)/n$	tetragonal, $P4(2)/n$	monoclinic, $P2(1)/c$	monoclinic, $C2/c$
a (Å)	15.594(4)	20.780(3)	21.744(4)	13.286(2)	14.443(1)	20.604(2)	22.404(8)
b (Å)	16.407(4)	18.755(3)	14.088(2)	29.145(4)	14.443(1)	11.2743(9)	18.590(7)
c (Å)	21.718(5)	12.126(2)	19.271(3)	22.784(3)	12.267(2)	44.294(3)	31.758(9)
β (deg)	96.970(6)	99.509(2)	91.715(3)	103.602(2)		91.725(1)	109.107(7)
V (Å ³)	5516(2)	4661(1)	5901(2)	8575(2)	2258.7(5)	10285(1)	12499(8)
Z	2	4	4	4	2	8	4
radiation (K α Å)	0.71073	0.71073	0.71073	0.71073	0.71073	0.71073	0.71073
T (K)	203(2)	203(2)	238(2)	203(2)	296(2)	203(2)	238(2)
D _{calcd} (g cm ⁻³)	1.317	1.344	1.305	1.451	1.164	1.347	1.080
μ_{calcd} (cm ⁻¹)	1.161	1.304	1.047	2.081	0.071	1.290	1.019
R, ^a R _w , ^b GoF	0.0923, 0.2264, 1.035	0.0597, 0.1434, 1.040	0.0553, 0.1263, 1.066	0.0336, 0.0856, 1.006	0.0751, 0.2179, 1.057	0.0855, 0.2680, 1.051	0.0975, 0.2663, 1.073

$$^a R = \sum |F_o| - |F_c| / \sum |F_o|, \quad ^b R_w = [(\sum |F_o| - |F_c|)^2 / \sum w(F_o)^2]^{1/2}.$$

Table 2. Selected Bond Distances (Å) and Angles (deg)

2	3	4	5
N(1)–N(1a) = 1.08(3)	Sm–O(3) = 2.630(6)	Sm–N(1) = 2.640(7)	N(1)–N(2) = 1.502(5)
Sm–N(1) = 2.880(18)	Sm–N(2) = 2.855(6)	Sm–N(3) = 2.696(7)	Sm(1)–N(1) = 2.249(4)
Sm–N(1a) = 2.974(18)	Sm–C(11) = 2.901(8)	Sm–N(2) = 2.974(7)	Sm(1)–N(2) = 2.253(4)
Sm–N(3) = 2.84(2)	Sm–C(12) = 2.956(8)	Sm–C(11) = 2.996(8)	Sm(2)–N(1) = 2.355(4)
Sm–C(11) = 2.90(2)	Sm–C(14) = 2.892(8)	Sm–C(12) = 2.979(9)	Sm(2)–N(2) = 2.370(4)
Sm–C(13) = 2.93(3)	Sm–N(1) = 2.601(6)	Sm–C(13) = 2.997(9)	Sm(3)–N(1) = 2.398(4)
Sm–C(14) = 2.85(3)	Li(2)–N(1) = 2.152(16)	Sm–C(14) = 2.983(8)	Sm(3)–N(2) = 2.376(4)
Sm–N(2) = 2.573(19)	Li(2)–C(1) = 2.167(17)	Sm–O(2) = 2.793(6)	Li(1)–N(1) = 1.904(9)
Sm–N(4) = 2.68(2)	Li(2)–C(2) = 2.242(17)	O(1)–Li(1) = 1.858(16)	Li(2)–N(2) = 1.915(9)
Li(1)–Cl = 2.18(6)	Li(2)–C(3) = 2.248(18)	O(1)–Li(2) = 1.897(17)	Sm(1)–N(1)–Sm(2) = 101.42(15)
Li(2)–Cl = 2.09(5)	Li(2)–C(4) = 2.177(17)	O(1)–Li(3) = 1.831(17)	Sm(1)–N(2)–Sm(2) = 100.87(15)
Li(3)–Cl = 2.14(6)	Li(1)–C(23) = 2.410(19)	O(1)–C(41) = 1.405(11)	Sm(1)–N(1)–Sm(3) = 98.52(15)
	Li(1)–C(24) = 2.275(18)	C(41)–C(42) = 1.372(14)	Sm(1)–N(2)–Sm(3) = 99.08(15)
	Li(1)–O(2) = 1.871(16)	O(1)–C(41)–C(42) = 117.5(9)	Sm(2)–N(1)–Sm(3) = 128.52(16)
	Li(2)–O(2) = 1.826(16)	O(2)–Sm–O(3) = 67.32(19)	Sm(2)–N(2)–Sm(3) = 128.89(17)
	Li(3)–O(2) = 1.933(14)	Li(1)–O(1)–Li(2) = 110.6(9)	
	O(2)–C(41) = 1.425(8)	Li(1)–O(1)–O(3) = 99.0(9)	
	C(41)–C(42) = 1.326(14)	Li(2)–O(1)–O(3) = 105.0(9)	
	O(2)–C(41)–C(42) = 122.1(9)		
6	7	8	
Li–N(1) = 2.386(13)	Sm(1)–Cl(1) = 3.15(2)	Sm–O(1) = 2.0685(12)	
Li–N(1a) = 2.045(12)	Sm(1)–N(2) = 2.457(9)	Sm–N(1) = 2.566(17)	
Li–O(1) = 1.971(13)	Sm(1)–N(4) = 2.405(8)	Sm–N(4) = 2.789(14)	
Li–C(1) = 2.246(12)	Sm(1)–N(3) = 2.778(9)	Sm–C(31) = 2.848(18)	
Li–C(2) = 2.306(12)	Sm(1)–C(21) = 2.818(10)	Sm–C(32) = 2.843(19)	
Li–C(3) = 2.455(13)	Sm(1)–C(22) = 2.839(10)	Sm–C(33) = 2.888(19)	
Li–C(4) = 2.488(13)	Sm(1)–C(23) = 2.818(10)	Sm–C(34) = 2.823(19)	
	Sm(1)–C(24) = 2.804(10)	Li(3)–N(4) = 2.10(5)	
	Li(1)–N(1) = 2.03(2)	Li(1)–N(3) = 2.64(5)	
	Li(1)–Cl(2) = 2.27(2)	Li(1)–C(21) = 2.55(5)	
	Cl(1)–Sm(1)–N(2) = 113.9(9)	Li(1)–C(22) = 2.30(5)	
	Cl(1)–Sm(1)–N(4) = 117.9(9)	Li(1)–C(23) = 2.21(5)	
	N(2)–Sm(1)–N(4) = 128.2(3)	Li(1)–C(24) = 2.44(5)	
	Li(1)–Cl(2)–Li(2) = 114.2(8)	Li(1)–Cl = 2.29(4)	
	Li(1)–Cl(2)–Li(3) = 110.6(8)	Sm–O(1)–Sm(a) = 176.5(6)	
	Li(2)–Cl(2)–Li(3) = 100.5(8)	Li(1)–Cl–Li(3) = 101.2(16)	
		Li(1)–Cl–Li(2) = 111.8(15)	
		Li(2)–Cl–Li(3) = 103.8(14)	

Scheme 1



it was possible to obtain a data file sufficient to elucidate the connectivity (Figure 1). The complex, formulated as $[(\text{--CH}_2\text{--})_5\text{--calix-tetrapyrrole}]\text{Sm}[\text{Li}(\text{THF})_3(\mu^3\text{--Cl})]_2\cdot$

$(\mu\text{--N}_2)\cdot 2\text{THF}$, is dinuclear and is formed by two samarium calix-tetrapyrrole moieties side-on coordinated to opposite sides of one dinitrogen molecule.⁴ Three

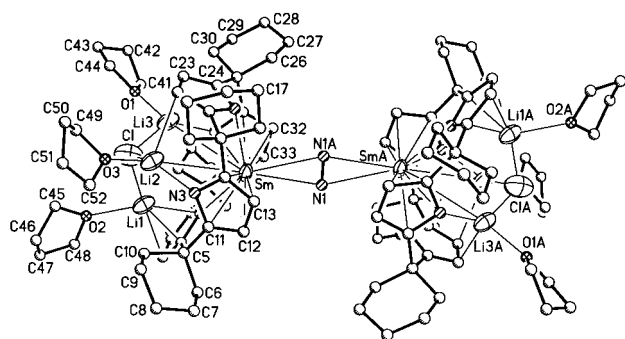


Figure 1. ORTEP drawing of **2**. Thermal ellipsoids are drawn at the 30% probability level. Bond distances are in angstroms and angles in degrees.

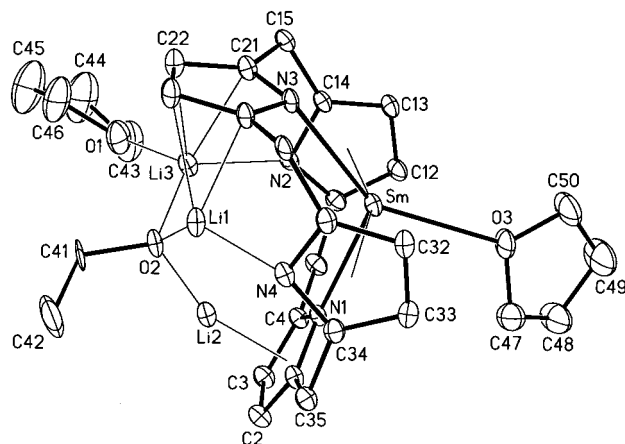


Figure 2. ORTEP drawing of **3**. Thermal ellipsoids are drawn at the 30% probability level. Bond distances are in angstroms and angles in degrees. Cyclohexyl groups attached to the ring have been omitted for clarity.

lithium atoms bridged by one chlorine are located on the exterior of each calix-pyrrole moiety pointing away from the Sm_2N_2 core and are linked to the ligand pyrrole rings by both π - and σ -bonding interactions. The N–N distance [$\text{N}(1)–\text{N}(1a) = 1.08(3) \text{ \AA}$] is very short and, within experimental error, is in the same range as the values determined by Evans in the labile decamethylsamarocene dinitrogen complex⁴ as well as by Scott in the labile U complex.¹⁶ The labile fixation and the shortness of the N–N distance, indicative of a minimal extent of perturbation of the N–N triple bond, is in sharp contrast with the side-on bonding mode, typically expected to afford a substantial degree of dinitrogen reduction.¹⁷

The second crystalline compound **3** present in the crude reaction mass is a Sm(II) enolate derivative $\{[(-\text{CH}_2-)_5]_4\text{-calix-tetrapyrrole}\}\text{Sm}(\text{THF})\text{Li}_2[\text{Li}(\text{THF})](\mu^3\text{-OCH=CH}_2)$ (Figure 2). The preparation of analytically pure **3** was conveniently performed in 47% yield upon exposing a solid sample of **1** to vacuum, followed by recrystallization from toluene. The complex is monomeric and possesses a structure closely related to that of the divalent **1**,¹² the major difference being the presence of an enolate group (from THF cleavage)¹⁸ bridging the three lithium atoms instead of the bridging

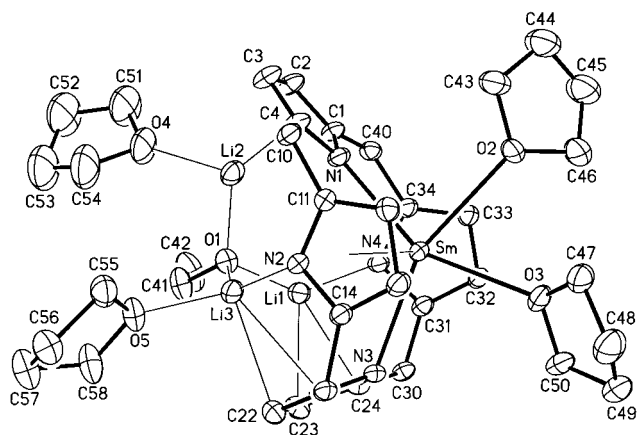


Figure 3. ORTEP drawing of **4**. Thermal ellipsoids are drawn at the 30% probability level. Bond distances are in angstroms and angles in degrees. Cyclohexyl groups attached to the ring have been omitted for clarity.

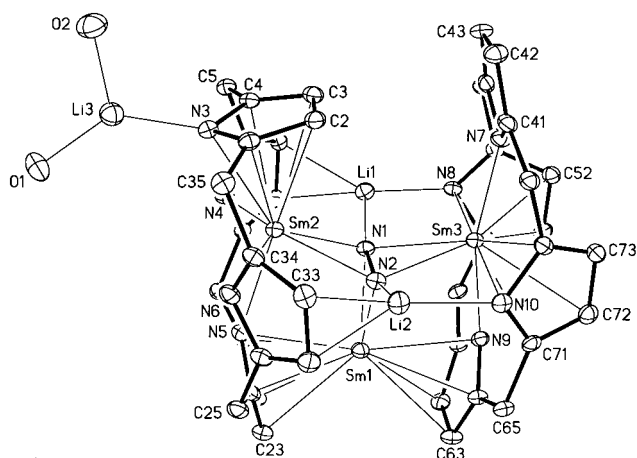


Figure 4. ORTEP drawing of **5**. Thermal ellipsoids are drawn at the 30% probability level. Bond distances are in angstroms and angles in degrees. Cyclohexyl groups attached to the ring have been omitted for clarity.

chlorine. As well, the severe bending of the $\text{O}_{\text{enolate}}–\text{Sm}–\text{O}_{\text{THF}}$ vector [$\text{O}(2)–\text{Sm}–\text{O}(3) = 150.4(2)^\circ$] is comparable to that present in the crystal structure of the dark green **1**.¹² The red color of the single crystals is most unusual for the +2 oxidation state of samarium. Similar to the case of the dinitrogen complex **2** however, red crystals of **3** also formed solutions with the characteristic dark green color in both THF and ether. The magnetic moment of **3** is also in agreement with the divalent samarium formulation.

The formation and coordination of an enolate group is a rather recurrent feature in the chemistry of the derivatives of this particular ligand system.^{18a,d–g} The enolate arises from a one-electron attack on one of the THF α -hydrogens. In this particular case, the electron can only be provided by the one-electron oxidation at

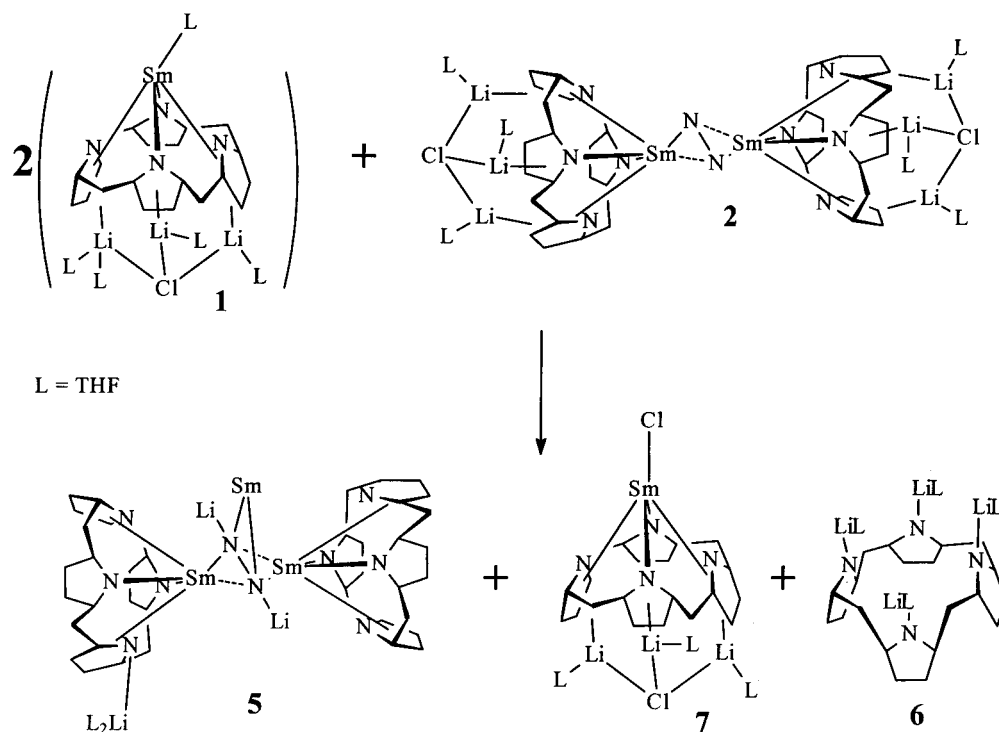
(15) Blessing, R., *Acta Crystallogr.* **1995**, A51, 33–3.

(16) Roussel, P.; Scott, P. *J. Am. Chem. Soc.* **1998**, 120, 1070.

(17) K. G. B. Clentsmith, F. G. H. Cloke *J. Am. Chem. Soc.* **1999**, 121, 10444. (b) Cohen, J. D.; Mylvaganam, M. Fryzuk, M. D.; Lohar, T. M. *J. Am. Chem. Soc.* **1994**, 116, 9529.

(18) (a) Jubb, J.; Gambarotta, S.; Duchateau, R.; Teuben, J. *J. Chem. Soc., Chem. Commun.* **1994**, 2641. (b) Aspinall, H. C.; Tillotson, M. R. *Inorg. Chem.* **1996**, 35, 2163. (c) Evans, W. J.; Dominguez, R.; Hanusa, T. P. *Organometallics* **1986**, 5, 1291. (d) Jubb, J.; Gambarotta, S. *Inorg. Chem.* **1994**, 33, 2503. (e) Jubb, J.; Gambarotta, S. *J. Am. Chem. Soc.* **1993**, 115, 10410. (f) Dubé, T.; Gambarotta, S.; Yap, G. P. A. *Organometallics* **1998**, 17, 3967. (g) De Angelis, S.; Solari, E.; Floriani, C.; Chiesi-Villa, A. *J. Chem. Soc., Dalton Trans.* **1994**, 2467. (h) Rupp, K. B.; Gambarotta, S.; Bensimon, C.; Yap, G. P. A. *Inorg. Chim. Acta* **1998**, 280, 143.

Scheme 2



the expenses of some of the divalent samarium centers. The abstraction of one hydrogen atom, eventually released as elemental hydrogen, is typically accompanied by the formation of an equivalent amount of ethylene (identified in the gas-chromatogram of the reaction mother liquor).

Once formed, complex 3 does not react with dinitrogen. At first glance this may seem surprising. On the other hand, the enolate group is bridging three lithium atoms which are either σ - or π -bonded to the same pyrrolyl rings which are in turn either π - or σ -bonded to the samarium center. Thus, the factors affecting the coordination sphere of lithium are ultimately affecting the redox potential of the Sm center. This behavior was previously observed in the labile ethylene coordination on similar divalent Sm derivatives⁸ where the presence of a chloride or enolate bridging the three lithium atoms indeed determined the position of the ethylene complexation equilibrium. Furthermore, complex 3 can be

recrystallized from a toluene solution in good yield, but it generates the new species $\{[(-CH_2-)_5]_4\text{-calix-tetra-pyrrole}\}\text{Sm}(\text{THF})_2\{\text{Li}[\text{Li}(\text{THF})_2]_2\}(\mu^3\text{-OCH=CH}_2)\cdot\text{THF}$ (4) upon dissolving in THF (Scheme 1). The solid state structure of 4 (Figure 3) does not deserve any particular comment since it is similar to that of 3 except for the presence of two additional molecules of THF. The first is attached to one of the three lithium atoms, while the second is directly coordinated to samarium. This new divalent samarium compound was isolated from a dark emerald green solution as crystalline material possessing a very unusual *pale yellow* color. Pale yellow crystals of 4 also impart the characteristic dark green color to THF solutions, possibly indicating that substantial structural rearrangements are likely to occur in solu-

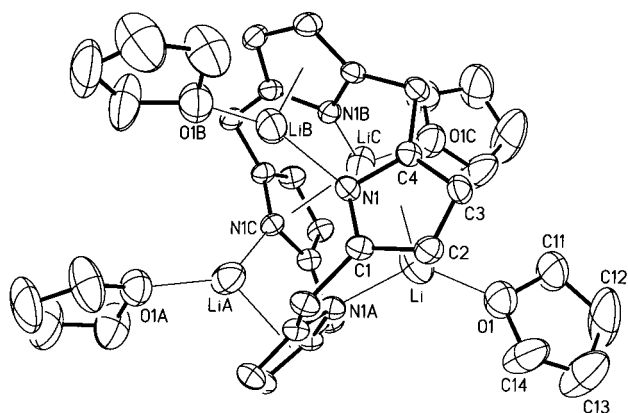


Figure 5. ORTEP drawing of 6. Thermal ellipsoids are drawn at the 30% probability level. Bond distances are in angstroms and angles in degrees. Cyclohexyl groups attached to the ring have been omitted for clarity reasons.

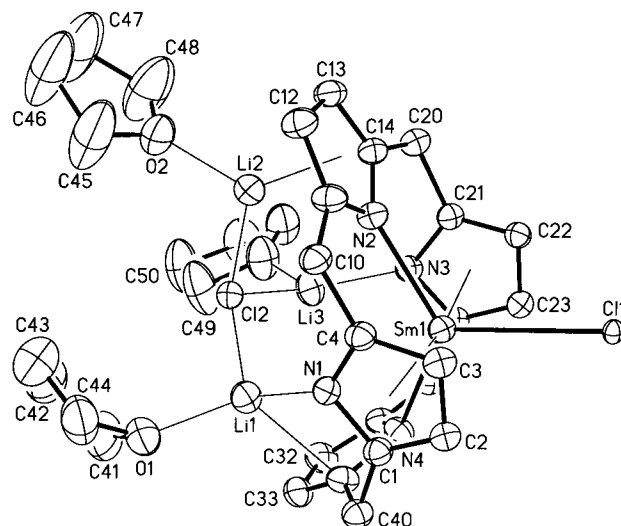


Figure 6. ORTEP drawing of 7. Thermal ellipsoids are drawn at the 30% probability level. Bond distances are in angstroms and angles in degrees. Cyclohexyl groups attached to the ring have been omitted for clarity reasons.

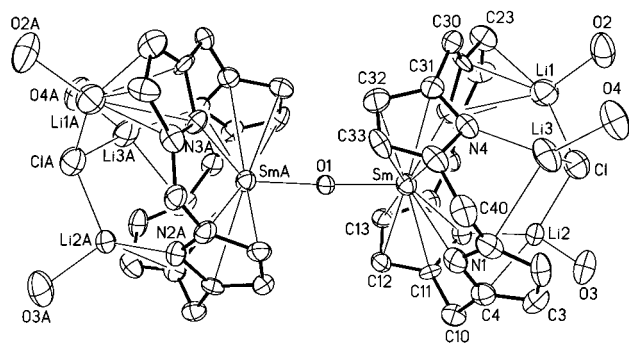


Figure 7. ORTEP drawing of **8**. Thermal ellipsoids are drawn at the 30% probability level. Bond distances are in angstroms and angles in degrees. Cyclohexyl groups attached to the ring have been omitted for clarity.

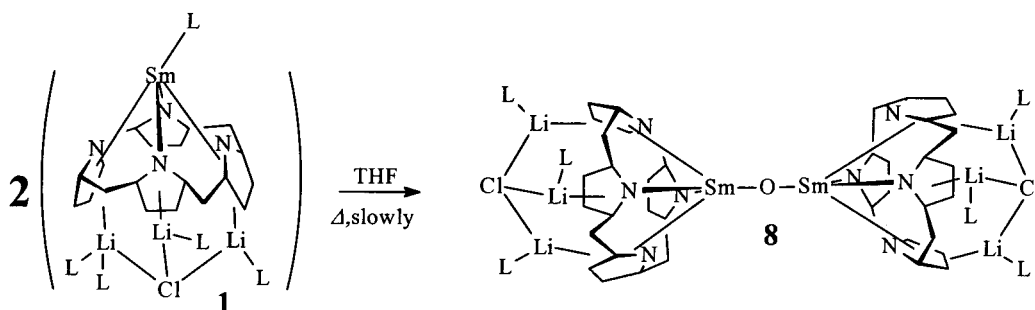
tion. Even in this case no evidence for reactivity toward dinitrogen was found.

When a dark green solution of **1** in THF was concentrated to small volume and stored for a few days under N_2 and at room temperature without exposure to hexane, orange-red flat crystals of a new dinitrogen complex $[\{ [(-CH_2)_5]_4\text{-calix-tetrapyrrole} \}_2\text{Sm}_3\text{Li}_2 \} (N_2)]$

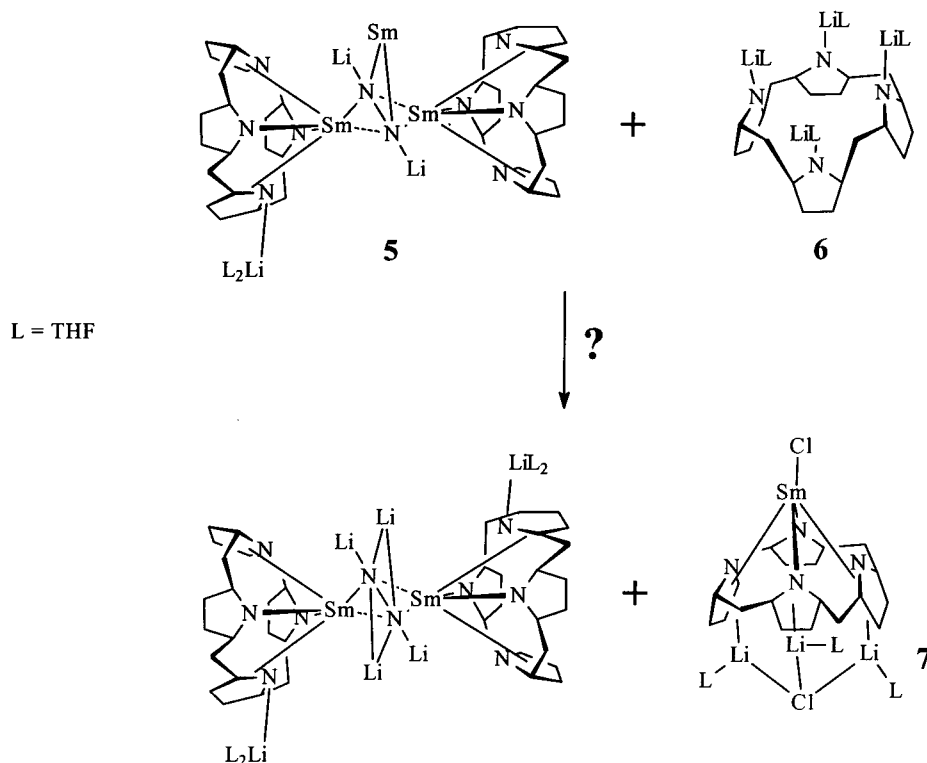
$[\text{Li}(\text{THF})_2] \cdot \text{THF}$ (**5**) separated in about 53% yield. The product was contaminated by a small amount of green crystals of unreacted **1**, which were easily removed by washing with toluene at room temperature. Complex **5** is thermally robust and, contrary to **2**, did not decompose even in boiling toluene. The complex is formed by two (calix-tetrapyrrole)Sm units side-on bonded to the same dinitrogen molecule and adopting an arrangement similar to that of complex **2** (Figure 4). However, a third Sm atom is located on the plane perpendicular to that of the Sm_2N_2 unit and is also side-on bonded to the dinitrogen moiety. This third Sm atom is in turn π -bonded to two parallel pyrrolyl rings, each from one ligand, thus forming a samarocene-type of structure. Two Li atoms located along the N–N axis, bridge two pyrrole rings from the two (calix-tetrapyrrole)Sm moieties. A third lithium atom is located at the exterior of the molecule connected to one nitrogen atom of one pyrrole ring of one of the two (calix-tetrapyrrole)Sm units.

The N–N distance $[\text{N}(1) \cdots \text{N}(2) = 1.502(5) \text{ \AA}]$ and the robustness of the complex imply that the N_2 molecule in complex **5** has undergone a four-electron reduction¹⁹

Scheme 3



Scheme 4



and that each Sm atom is in the +3 oxidation state. Furthermore, the fact that the complex contains only *two* ligands and *three* samarium atoms implies that during the reaction one calix-tetrapyrrole has been demetalated. From the stoichiometry point of view, the formation of **5** may be regarded as the result of the *formal* addition of two molecules of **1** to the dinuclear **2** (Scheme 2). In order for **5** to be formed, the reaction requires the elimination of LiCl, of $\{[(-CH_2-)_5]_4\text{-calix-tetrapyrrole}\}[\text{Li}(\text{THF})]_4$ (**6**) [isolated in 15% yield from the mother liquor and identified by X-ray crystallography (Figure 5)], and of the trivalent samarium complex $\{[(-CH_2-)_5]_4\text{-calix-tetrapyrrole}\}\text{Sm}(\text{Cl})[\text{Li}(\text{THF})]_3(\mu^3\text{-Cl})$ (**7**). This latter species was isolated in minimal yield from the reaction mixture. Fortunately the crystallinity was sufficient to undertake a structural determination (Figure 6). The complex was subsequently prepared in good yield through direct synthesis from $\text{SmCl}_3(\text{THF})_3$ starting material.

Finally, we observe that a tiny amount of colorless crystals of a new compound (**8**) could be obtained from the mother liquors of the preparation of both **2** and **5**. This new product, revealed as a dinuclear oxo-bridged $\{[(-CH_2-)_5]_4\text{-calix-tetrapyrrole}\}\text{Sm}[\text{Li}(\text{THF})]_3(\mu^3\text{-Cl})_2(\mu\text{-O})$ (**7**) by an X-ray crystal structure (Figure 7), was obtained in significant yield when one reaction solution was evaporated to dryness and separately extracted with boiling portions of hexane, toluene, and THF. Colorless crystals of **8** were obtained from the THF extracts. The structure is closely reminiscent of that of **2** except for the replacement of the bridging dinitrogen by a bridging oxygen. The origin of the bridging oxygen atom is likely to be ascribed to a two-electron attack on a THF molecule occurring slowly and irreversibly in the solutions of these divalent samarium compounds (Scheme 3).

Concluding Remarks

By using the $\{[(-CH_2-)_5]_4\text{-calix-tetrapyrrole}\}$ ligand system, it was possible to isolate two new dinitrogen complexes of very different nature. The "labile" **2** is the result of simple replacement in complex **1** of the coordinated THF by dinitrogen, and it can be isolated only in hexane/THF mixtures where the solubility of this particular complex is severely decreased. Conversely, the formation of the trinuclear **5** is a more complex process arising from four-electron reduction of dinitrogen obviously achieved via involvement of four Sm(II) centers on the same dinitrogen molecule. At this stage it is tempting to speculate that the *dinuclear* samarium complex $[(\text{Et}_8\text{-calix-tetrapyrrole})\text{SmLi}]_2\text{Li}_4\text{N}_2$ reported before⁵ may be generated by a similar sequence of reactions, the final step being the attack of the $(\text{Et}_8\text{-calix-tetrapyrrole})[\text{Li}(\text{THF})]_4$ intermediate on the analogue of **5** (Scheme 4). Simple replacement of one trivalent Sm atom with three lithium cations may afford the final dinuclear dinitrogen complex containing a dinitrogen moiety reduced by four-electron reduction and encapsulated inside a Sm_2Li_4 cage.

Finally, similar to the case of the reversible ethylene coordination promoted by the same complexes, the nature of the group bridging the three lithium atoms at the periphery of the molecule is critical for dinitrogen fixation since simple replacement with enolate, obtained during competitive THF cleavage process, gave only unreactive Sm(II) species.

Acknowledgment. This work was supported by the Natural Sciences and Engineering Council of Canada (NSERC) and NATO.

Supporting Information Available: Listings of atomic coordinates, thermal parameters, and bond distances and angles for all the complexes. This material is available free of charge via the Internet at <http://pubs.acs.org>.

OM000698P

(19) (a) Fryzuk, M. D. *Coord. Chem. Rev.* **2000**, 200–202, 379.
(b) Bazhenova, T. A.; Shilov, A. E. *Coord. Chem. Rev.* **1995**, 144, 69.